Agilent

Trusted Answers

Kinetic Fluorescence Live Cell Assays

Application Compendium

Table of Contents

Introduction 3

Fluorescent probes 4

Fluorescent proteins 5

Instrumentation 6

Kinetic Fluorescence Live Cell Assays 7

Detecting cell cycle phase through the incorporation of cell cycle/fluorescent protein fusions 7

Kinetic live cell imaging of apoptosis and necrosis 9

Characterizing calcium mobilization using kinetic live cell imaging 11

2D scratch wound healing analysis of a co-cultured cell model 13

Monitoring mitochondrial dynamics via live cell imaging 15

Conclusion 18

References 18

Introduction

Living organisms, composed of multiple different tissues and cell types, are highly dynamic in nature. Imaging in a live cell format is therefore a critical tool for laboratories across a wide variety of research disciplines. The methods in which cells have been studied has seen many changes since Antonie van Leeuwenhoek first used a microscope to observe blood flow in the capillaries of the ears of living rabbits in the 17th century.[1, 2] A vast number of early cellular analyses were performed as an end point experiment, where cells are incubated with a test molecule for a designated amount of time before a microplate read or imaging step is performed to determine the effect. While providing an easy to follow protocol, many times the true effect of a treatment, as expressed by an accurate EC_{50} value (Figure 1), can be missed if the incubation period is too short or too long.

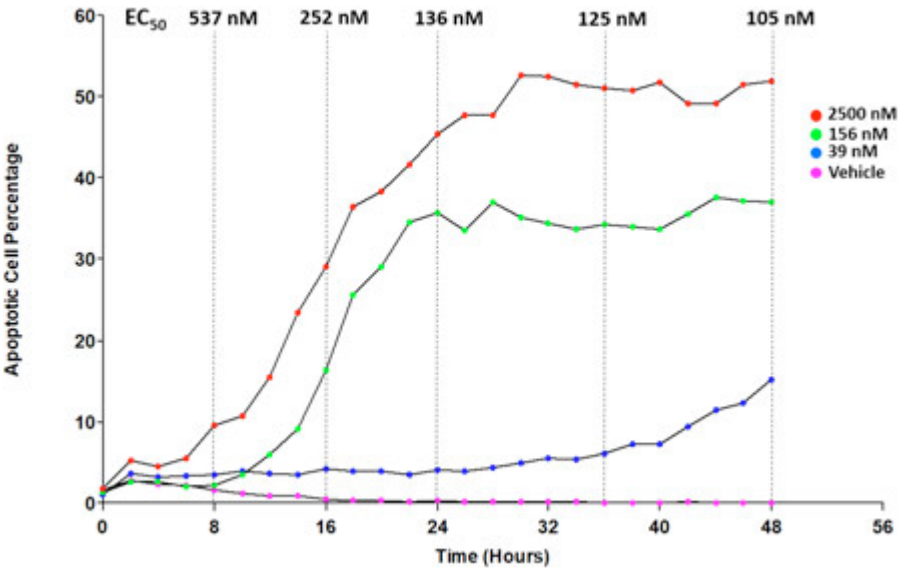

Figure 1. Apoptotic cell percentages determined from kinetic monitoring of variable concentrations of camptothecin incubated with HT1080 cells. EC_{50} values calculated from each area under the curve for the full drug titration following 8, 16, 24, 36, and 48 hour incubations.

Evaluating treatment effects on test cell models using kinetic assays, where monitoring is performed throughout the entire incubation period, provides greater biologically relevant insight into cellular responses (Figure 1). In addition to being able to detect signal modulations from a cellular event over time, kinetic imaging assays also allow for observations of changes in cellular morphology and phenotype. The combination of both types of information yields a more holistic approach to fully understand the effects that molecules have on the cells. Kinetic imaging can also be used to determine appropriate incubation times for incorporation into downstream higher throughput end point assays. This technique has led to a number of discoveries, including proving the existence of hemogenic endothelium[3, 4, 5], demonstration of lineage instruction by cytokines[6], as well as numerous breakthroughs in the fields of neurogenesis[7, 8, 9, 10], and immunology.[11, 12, 13]

Furthermore, the combination of kinetic live imaging with conventional fluorescence microscopy techniques has become an integral part of cellular analysis methodologies. Fluorescence imaging relies on illumination of fluorescent molecules with a defined wavelength of light ideally near the peak of the fluorophore excitation spectrum, and detection of light emitted at a longer wavelength. Commonly used live cell fluorescent molecules, such as fluorescent probes or dyes, and fluorescently labeled proteins have provided a range of tools to investigate virtually any cellular process of interest.

Fluorescent probes

A wide range of fluorescent probes have been developed for use in live cell kinetic imaging. These can broadly be divided into probes that 1) stain entire cells or intracellular structures for identification purposes, 2) track changes to a specific cellular structure, or 3) track phenotypic changes within a cell.

The first category of fluorescent probes are designed to label entire cells or subcellular organelles for enumeration. Examples include dyes such as DRAQ5 (Biostatus Limited, Leicestershire, UK), MitoTracker (Thermo Fisher Scientific, Waltham, MA) and Cytopainter (Abcam, Cambridge, UK) which label nuclei, mitochondria, and lysosomes, respectively. Whereas CellTracker dyes (Thermo Fisher Scientific, Waltham, MA), label the entire cell for easy identification.

The second set of probes is used to track changes to a particular cellular organelle. One of the most common events this type of probe is used for detects changes in mitochondrial membrane potential. Probes such as the cell permeable TMRE accumulate in active mitochondria with high membrane potential, while, depolarized or inactive mitochondria with decreased membrane potential fail to sequester TMRE.

Finally, a large number of probes have been developed to track a variety of phenotypic cellular events such as apoptosis, necrosis, autophagy, and oxidative stress. Here probes produce a fluorescent signal in response to phenotypic changes.

For instance, fluorogenic apoptotic probes either bind to molecules present during stages of apoptosis, such as external exposure of phosphatidylserine, or are cleaved by these molecules, such as cleavage by caspase-3 to create a fluorescent final product. Necrosis probes such as propidium iodide are non-permeable cellular dyes, and therefore, only after the cell membranes of necrotic cells are compromised can the dye enter the cells, bind to cellular nucleic acids, and create a fluorescent signal.

Fluorescent proteins

While the bulk of kinetic fluorescence live cell imaging is typically accomplished through the use of fluorescent probes, incorporation of genetically encoded fluorescent protein tags (fluorescent proteins) also plays a vital role. Prasher and colleagues[14] first reported the cloning of green fluorescent protein (GFP) from Aequorea victoria, eventually leading to the 2008 Nobel Prize in Chemistry. Over the last decades dozens of fluorescent proteins have been engineered with excitation and emission spectra spanning from the ultraviolet to near infrared range of the visible spectrum imaging.[15, 16, 17, 18] Not only can fluorescent proteins be engineered to emit different color signals, they can be targeted to specific subcellular locations, such as the nucleus, nuclear membrane, or mitochondria. The wide range of spectral properties and the ability to direct their localization makes these proteins ideal for use in multiplexed cellular assays, as a variety of targeted and phenotypic phenomena can be tracked at the same time.

The incorporation of kinetic live cell fluorescence imaging provides an ideal method to monitor a wide range of cellular phenomena that can take place over seconds, hours, days, or even weeks. In the remaining portion of this application compendium we describe how different fluorescent kinetic live cell assay procedures can be optimized and performed using the Agilent BioTek cellular imaging and automation instrumentation.

Instrumentation

Agilent BioTek Lionheart FX automated microscope

Lionheart FX automated microscope is a compact, inclusive microscopy system for a broad range of imaging workflows. It has up to 60x air; 60x and 100x oil immersion magnification, with fluorescence, brightfield, color brightfield, and phase contrast channels for maximum application reach. Environment controls including incubation to 40 °C, CO_2/O_2 control and a humidity chamber optimize conditions for kinetic live cell imaging applications.

Agilent BioTek Cytation 7 cell imaging multimode reader

Cytation 7 cell imaging multimode reader combines automated digital upright and inverted widefield microscopy with conventional multimode microplate reading. The inverted microscope provides sample visualization from 1.25x to 60x magnification in fluorescence, brightfield and color brightfield; the upright microscope with reflected light imaging enables applications such as ELISpot or fast slide scanning and ROI detection workflows.

Agilent BioTek Cytation 5 cell imaging multimode reader

Cytation 5 cell imaging multimode reader combines automated digital microscopy and conventional microplate detection in a configurable, upgradable platform. The microscopy module offers up to 60x magnification in fluorescence, brightfield, high contrast brightfield, color brightfield and phase contrast imaging; temperature control to 65 °C and CO_2/O_2 control facilitate live cell imaging workflows.

Agilent BioTek BioSpa live cell analysis system

BioSpa live cell analysis system is configured with the Agilent BioTek automated incubator and Agilent BioTek cytation imager to automate kinetic live cell analysis workflow in up to 8 microplates or other labware. Temperature and CO_2/O_2 control, plus humidity monitoring support live cell imaging workflows. Liquid handling can be integrated for further process automation.

Agilent BioTek Autoscratch wound-making tool

The AutoScratch wound-making tool automatically creates reproducible scratch wounds in cell monolayers grown in microplates. The simple pushbutton operation and tool-free scratch pin manifold exchange make it easy to process either 96- or 24-well plates, which are commonly used in migration and invasion assays. The compact system features an onboard, pre-programmed cleaning routine to keep the scratch pins free of cell buildup and avoid contamination.

Kinetic Fluorescence Live Cell Assays

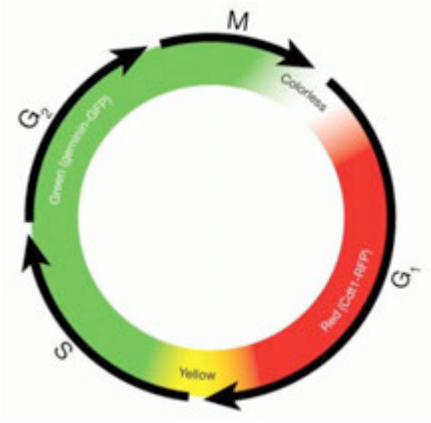

Figure 2. Dynamic color change of Premo FUCCI cell cycle sensor. FUCCI is a fluorescent, two-color sensor of cell cycle progression and division in live cells. Cells change from red in the G1 to yellow in the G1/S interphase and green in S, G2, and M phases, as geminin and Cdt1, fused to one green and red fluorescent proteins respectively are expressed at specific points in the cell cycle.

Detecting cell cycle phase through incorporation of cell cycle/fluorescent protein fusions

Assay principle

The Premo Fluorescence ubiquitination cell cycle indicator (FUCCI) technology (Thermo Fisher Scientific, Waltham, MA) is based on two cell cycle-regulated proteins, geminin and Cdt1, fused to a green (emGFP) and red (TagRFP) fluorescent protein, respectively.[19] As Cdt1 and geminin are present only during specific phases of the cell cycle, the fluorescent protein chimeras are similarly dependent. Ubiquitination by specific ubiquitin E3 ligases target the chimeric constructs for degradation and display temporal regulation of activity, resulting in the cycling of geminin and Cdt1 levels during the cell cycle. Geminin-GFP is degraded in the G1 phase, while the presence of Cdt1-TagRFP is indicated by red fluorescence within nuclei. During the S, G2, and M phases, Cdt1- TagRFP is degraded and only geminin-GFP remains, resulting in green-fluorescent nuclei. During the G1/S transition, when Cdt1 levels are decreasing and geminin levels are increasing, both proteins are present, giving a yellow-fluorescent nuclear signal. This cyclical color change (red to yellow to green) can be used to track progression through the cell cycle and division (Figure 2).

Method summary

Following transfection with the FUCCI sensor using BacMam 2.0, and treatment with potential cell cycle inhibitors, cells are kinetically monitored for cell cycle progression by capturing images every 90 minutes using a 4x objective and the high contrast brightfield, GFP, and RFP imaging channels of the Agilent BioTek cellular imagers. The high contrast brightfield channel captures total cells within an image, while the GFP channel captures cells in the S, G2, and M phases, and the RFP channel captures cells in the G1 and S phases.

Analysis and results

Following capture, all images are pre-processed to remove background signal (Figure 3A). Then using the change in signal in the high contrast brightfield channel, primary object masks are automatically placed around all cells in the image (Figure 3B).

A

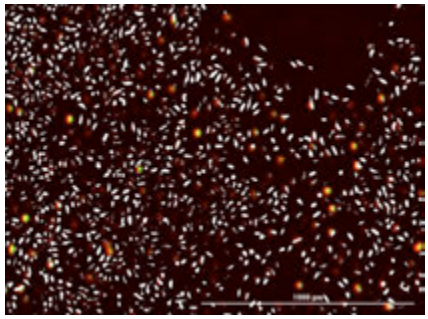

B

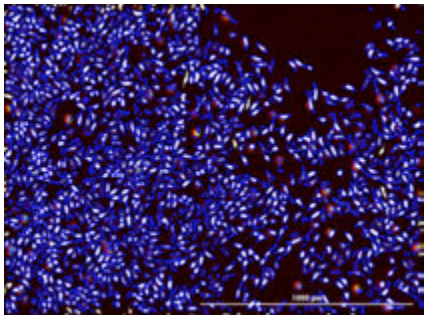

Figure 3. Overlaid pre-processed high contrast brightfield, GFP, and RFP images before (A) and after (B) object masks are applied through cellular analysis.

During secondary masking, primary masks are dilated to capture the GFP and RFP signal (Figure 4A). Subpopulation analyses were conducted to identify cells in the G1 or G2/M phases Cells with a minimum peak signal from the Cdt1-TagRFP protein, captured using the RFP imaging channel, within the secondary masks were identified as being in G1 (Figure 4B), while cells with a minimum peak signal from the Geminin-GFP protein within the secondary masks, captured using the GFP imaging channel, were identified as being in the G2/M phase (Figure 4C). During the S phase, when both cell cycle fusion proteins are present, cells appear yellow. To meet the criteria of bring in the S phase, cells had to meet the minimum peak signal from both proteins (Figure 4D).

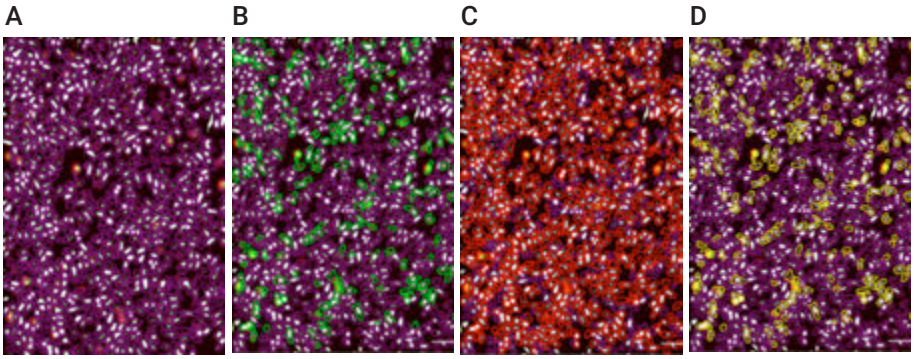

Figure 4. (A) Expanded primary masks during the secondary masking process. Subpopulations using peak RFP and/or GFP signals then identify cells in (B) G1; (C) G2/M; or (D) S cell cycle phases.

Following analysis, total, G1 (red), G2/M (green), and S (yellow) cell counts are then determined at each timepoint during the incubation period. Final red and green cell counts are calculated by subtracting the yellow cells from initial determined red or green cell numbers to avoid double counting (Figure 5A). Red, green, and yellow cell percentages are then computed by dividing subpopulation cell counts by the total cell value at each timepoint (Figure 5B). Final kinetic plots then reveal the stage of cell cycle arrest accomplished by the added compound.

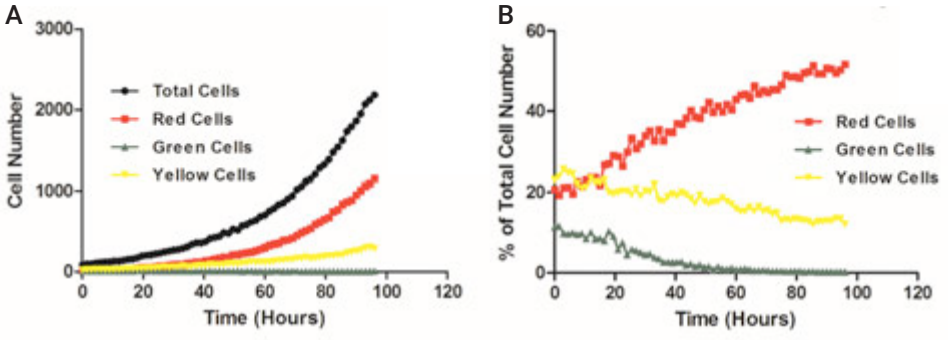

Figure 5. (A) Kinetic cell numbers counted for total, G1 (red), G2/M (green), and S (yellow) phase cells. (B) Percent of total cells for G1, G2/M, S cell cycle phase cells.

Recent publications using Agilent BioTek microscopes

1. Mehta, Sunali, et al. "Dephosphorylation of YB-1 Is Required for Nuclear Localisation During G2 Phase of the Cell Cycle." *Cancers, vol. 12, no. 2, Jan.* **2020**, *p. 315.* Doi: 10.3390/cancers12020315.
2. Van den Berg, Jeroen. Product of the Surrounding: Location Dependent Effects on DNA Double Strand Break Responses. Utrecht University, **2019**.

Kinetic live cell imaging of apoptosis and necrosis

Assay principle

The Kinetic Apoptosis Kit (Abcam, Cambridge, UK) is based on two separate technologies to detect apoptotic and necrotic cellular activity, respectively. pSIVA-IANDB (Polarity Sensitive Indicator of Viability & Apoptosis) is an Annexin XII-based polarity sensitive probe for the spatiotemporal analysis of apoptosis. External plasma membrane phosphatidylserine (PS) exposure is a hallmark phenomenon occurring early during apoptosis. When PS translocates to the outer membrane leaflet, binding of pSIVA-IANBD to PS can then occur. The IANBD labels are then exposed to the nonpolar lipid environment of the membrane which results in a 'switching on' of the IANBD green fluorescence signal. Propidium iodide (PI), as previously explained, is a fluorescent intercalating necrosis probe which is non-cell permeable. Only when cell membranes of necrotic cells are compromised can the dye enter the cells, bind to cellular nucleic acids, and create a fluorescent signal.

Method summary

The pSIVA-IANDB and PI fluorescent probes were added to media at concentrations of 10 µL/mL and 5 µL/mL, respectively, and used to create an 8-point titration of camptothecin ranging from 10,000 to 0 nM by serial 1:4 titrations. Media containing compound and probes was then added to wells containing 2000 HT-1080 cells per well. Cells were kinetically monitored for induction of apoptosis and necrosis by capturing images every 2 hours over a 48 hour time period using a 4x objective and the high contrast brightfield, GFP, and RFP imaging channels of the Agilent BioTek cellular imagers. The high contrast brightfield channel captures total cells within an image, while the GFP channel captures the green pSIVA-IANDB signal from apoptotic cells, and the RFP channel captures the PI signal from necrotic cells.

Analysis and results

Following capture, all images are pre-processed to remove background signal (Figure 6A). Then using the change in signal in the high contrast brightfield channel, primary object masks are automatically placed around all cells in the image (Figure 6B).

A

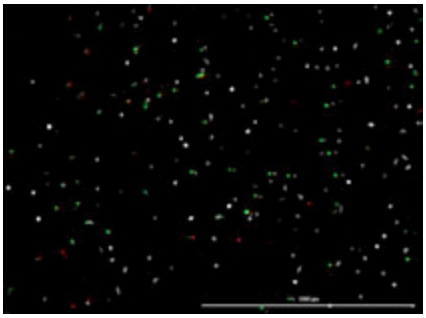

B

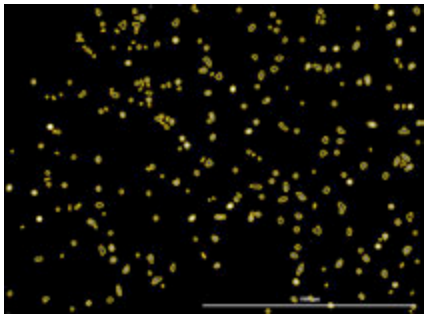

Figure 6. (A) Overlaid pre-processed high contrast brightfield, GFP, and RFP image. (B) High contrast brightfield image only showing object masks automatically applied using change in brightfield signal during cellular analysis.

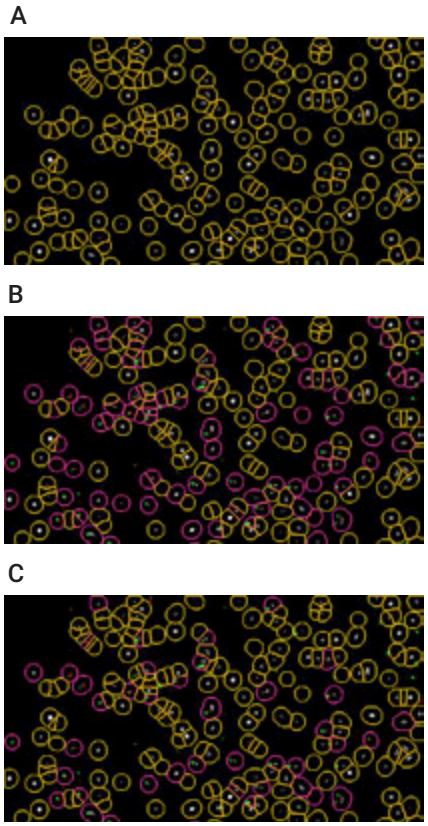

Figure 7. (A) Expanded primary masks during the secondary masking process. Subpopulations using integral GFP or RFP signals then identify (B) apoptotic; or (C) necrotic cells.

Figure 8. Kinetic percent (A) apoptotic; and (B) necrotic cell curves following 48 hour incubation of camptothecin (2500-0 nM) with HT-1080 cells. Area under the curve values then plotted in terms of camptothecin concentration to determine compound effectiveness to induce (C) apoptosis; or (D) necrosis.

During secondary masking, primary masks are dilated to capture the GFP and RFP signal (Figure 7A). To identify apoptotic or necrotic cells subpopulation analyses were conducted. Cells with a minimum integral signal from the pSIVAIANDB probe, captured using the GFP imaging channel, within the secondary mask were identified as being apoptotic (Figure 7B), while cells with a minimum PI integral signal, captured using the RFP imaging channel, within the secondary mask were identified as being necrotic (Figure 7C).

Following analysis, percent apoptotic and necrotic cells within each image at each timepoint is determined by dividing the apoptotic or necrotic cell numbers by the total number of cells counted per image, and expressing each value as a percentage. These values can then be plotted over time to visualize the effect that varying concentrations of the test molecule, in this case camptothecin, has to induce apoptosis (Figure 8A), and necrosis (Figure 8B) on the cell model. Using the kinetic plots, Agilent BioTek Gen5 can also calculate the area under each kinetic curve, generating one total area value for the curve corresponding to the concentration of camptothecin tested. These numbers can then be plotted in relation to camptothecin concentration to create an EC_{50} value demonstrating the ability of the compound to induce apoptosis (Figure 8C) and necrosis (Figure 8D).

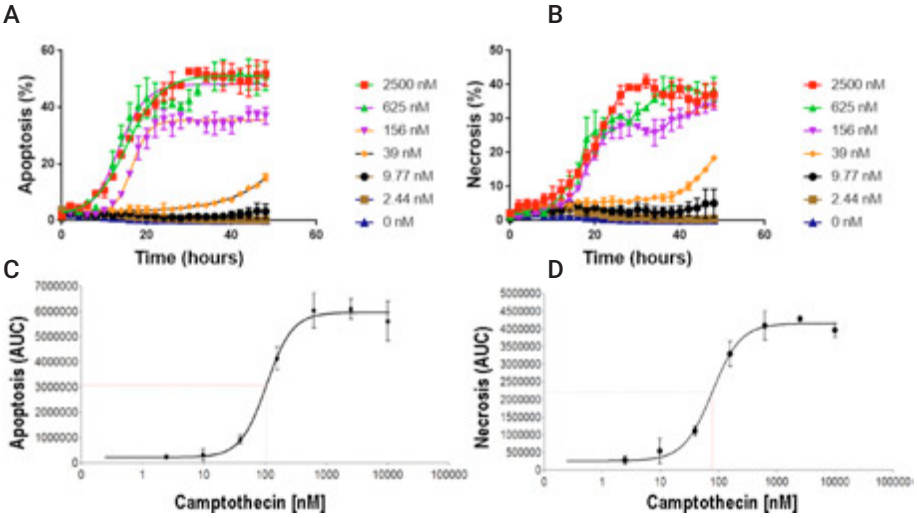

Recent publications using Agilent BioTek microscopes

1. Taabazuing, Cornelius Y., et al. "Pyroptosis and Apoptosis Pathways Engage in Bidirectional Crosstalk in Monocytes and Macrophages." *Cell Chemical Biology, vol. 24, no. 4,* Apr. **2017**, *pp. 507-514.e4.* Doi: 10.1016/j. chembiol.2017.03.009.
2. Akbarzadeh Khiavi, Mostafa, et al. "PEGylated Gold Nanoparticles-Ribonuclease Induced Oxidative Stress and Apoptosis in Colorectal Cancer Cells." *BioImpacts, vol. 10, no. 1,* July **2019**, *pp. 27–36.* Doi: 10.15171/bi.2020.04.
3. Filali, Samira, et al. "Live-Stream Characterization of Cadmium-Induced Cell Death Using Visible CdTe-QDs." *Scientific Reports, vol. 8, no. 1,* Dec. **2018**, *p. 12614.* Doi: 10.1038/s41598-018-31077-2.
4. Inde, Zintis, et al. Large-Scale Analysis of Cell Death Phenotypic Heterogeneity. *preprint, Cancer Biology,* 29 Feb. **2020**. Doi: 10.1101/2020.02.28.970079.

Characterizing calcium mobilization using kinetic live cell imaging

Assay principle

Mobilization of intracellular calcium stores following G protein coupled receptor (GPCR) activation is critical for cells to respond to intercellular and environmental cues. Binding of a signal molecule to a GPCR activates the associated trimeric GTP-binding protein (G protein), comprised of an α-subunit, and a β- and γ-subunit complex. Activation of the Gs and Gq sub-family of α-subunits triggers the release of intracellular calcium stores into the cytoplasm, which propagates the signal by regulating calcium-dependent proteins[20]. Fluo-4 is a calcium indicator that has been used extensively for detecting changes in calcium levels. Fluo-4 AM (Thermo Fisher Scientific, Waltham, MA) is an acetoxymethyl ester derivative of Fluo- 4 that can permeate cell membranes. Once the Fluo-4 AM molecule is inside the cell, nonspecific esterases cleave the lipophilic blocking groups, forming a charged compound that is less likely to leak out of cells. In the presence of calcium, the free Fluo-4 exhibits increased fluorescence at 494/506 nm.

Method summary

Fluo-4 AM, 4 µM, was added to plated cells and allowed to permeate the cells for one hour before unincorporated probe was removed and replaced with DPBS. The plate was then inserted into a BioTek imager where kinetic fluorescent imaging took place using a 4x objective and the GFP imaging channel at a rate of 3 frames per second. Baseline images were captured at this rate for a total of 5 seconds. At that time the in-line injectors were used to dispense ATP to a final concentration of 10 µM while the plate was still in the imaging position. Kinetic imaging then commenced at the same rate for an additional 30 seconds to monitor the effect on calcium signaling.

Analysis and results

Following capture, all images are pre-processed to remove background signal. Basal Fluo-4 signal from stained cells above background, as measured by the GFP channel, is used to place object masks around all cells (Figure 9A). In this manner, the total Fluo-4 signal from each cell is captured and quantified over the entire incubation period (Figure 9B). Total fluorescence from all objects within images following ATP stimulation is then divided by the total average total fluorescence from images of basal signal prior to stimulation to generate a normalized relative fluorescence ratio. When plotted over time, the level of calcium mobilization can then be observed (Figure 9C).

A

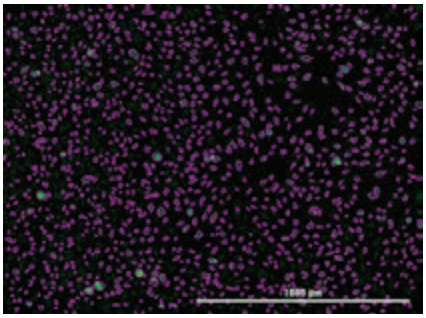

B

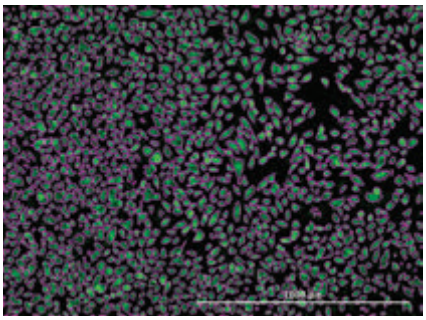

C

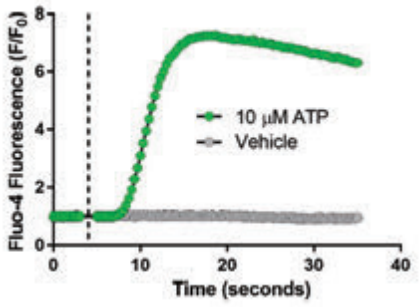

Figure 9. (A) 4x image of labeled cells prior to stimulation with object masks placed using basal Fluo-4 signal. (B) Fluo-4 signal within object masks at 15 seconds post ATP addition. (C) Kinetic plot of total Fluo-4 signal ratio over the entire length of the kinetic experiment. Dashed line illustrates time of ATP injection.

By placing a plug around a single cell in an image during Gen5 cellular analysis, such that only the signal from that cell is analyzed over the length of the kinetic experiment, resulting calcium flux can be characterized for individual cells (Figure 10A). Using this method, the rate of intracellular calcium release and the interval between spikes in calcium levels can be defined with high temporal resolution. The resulting activation profiles can be used to compare cellular responses under different conditions or between different cell types (Figure 10B).

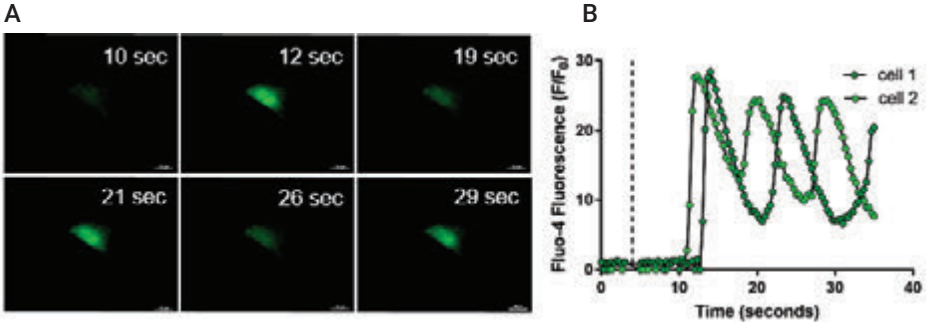

Figure 10. Single cell calcium mobilization characteristics. (A) Images of plug set around cell 2 at six time points. (B) Cells 1 and 2 exhibited similar activation profiles. A rapid spike in calcium mobilization occurred 5-7 seconds post ATP injection (10 µM final) (dashed line), followed by a gradual decline in Fluo-4 fluorescence over 6-8 seconds before calcium levels spiked again.

By adding a nuclear dye, such as Hoechst 33342, in addition to Fluo-4 AM (Figure 11A), calcium mobilization per cell can also be accomplished. Gen5 places primary masks around the nuclei of each cell within the image. Secondary masks are then placed around GFP captured signal from the Fluo-4 probe (Figure 11B). Total GFP signal within each secondary mask is quantified. Using a minimum total signal value to eliminate non-responsive cells within the image, the number of cells responding to stimulation is returned by Gen5. By dividing by the total number of cells within the image, determined by counting Hoechst 33342 stained cells, a percent responder cell value is calculated. This can then be plotted versus the concentration of stimulant, or inhibitor added to the well to determine the effectiveness of calcium mobilization.

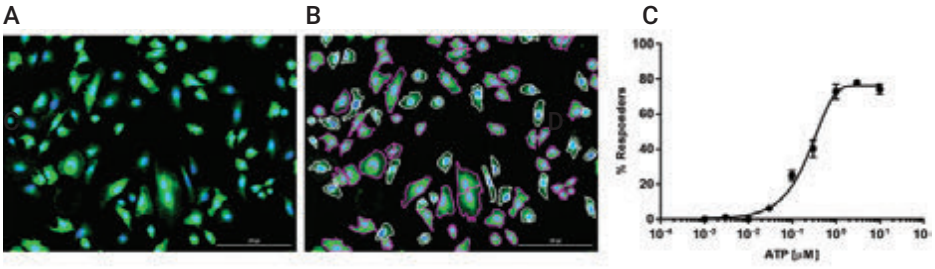

Figure 11. (A) 4x image of Hoechst 33342 and Fluo-4 stained cells. (B) Stained cells following ATP stimulation with primary nuclear masks using Hoechst 33342 signal and secondary masks using Fluo-4 signal. (C) Plot of percent responding cells per treatment demonstrating calcium mobilization effectiveness.

Recent publications using Agilent BioTek microscopes

1. Zhou, Wenqing, et al. "Mitofusin 2 Regulates Neutrophil Adhesive Migration and the Actin Cytoskeleton." *preprint, Cell Biology,* 13 Apr. **2019**. Doi: 10.1101/608091.
2. Harlen, Kevin M., et al. "Live-Cell Assays for Cell Stress Responses Reveal New Patterns of Cell Signaling Caused by Mutations in Rhodopsin, α-Synuclein and TDP-43." *Frontiers in Cellular Neuroscience, vol. 13,* Dec. **2019**, *p. 535,* Doi: 10.3389/fncel.2019.00535.
3. Jeon, Bo-Hui, et al. "Dexamethasone Treatment Increases the Intracellular Calcium Level Through TRPV6 in A549 Cells." *International Journal of Molecular Sciences, vol. 21, no.* 3, Feb. **2020**, *p. 1050*. Doi: 10.3390/jms21031050.

2D Scratch wound healing analysis of a co-cultured cell model

Assay principle

The wound healing or scratch assay is a straightforward and widely used method to measure cell migration. In the method, once cultured cells reach confluence, the monolayer is mechanically scratched, thus creating a cell-free zone, and for some cell models simulates a wound area. Collective cell migration into the cell-free zone is then kinetically imaged over time to characterize cell movement when uninhibited or under the influence of a test molecule. Stromal cells, such as fibroblasts, are responsible for depositing components of the ECM, and in the solid tumor microenvironment, influence cancer cells in migration, invasion and other tumorigenic processes.[21] Because of the important role that stroma plays *in vivo* these cells, in addition to target cancer cells, should be included when performing *in vitro* cell migration studies to increase the relevance of generated data. By having each co-cultured cell type express a separate fluorescent protein, it is easy to image and analyze individual relative kinetic wound healing rates within the co-culture cell model.

Method summary

GFP expressing U-87 glioblastoma and RFP expressing primary fibroblasts were diluted to concentrations of $3.0x10^5$ cells/mL, mixed in a 1:1 ratio, and added to wells of a 96-well plate. Following attachment to create a confluent cell monolayer, the plate was transferred to the AutoScratch tool where pins on the robotic arm created consistent cell free zones (scratches) within the cell layers of each well. Plates were then placed into the BioSpa 8, with atmospheric conditions previously set to 37 °C/5% CO_2. The BioSpa 8 software was programmed such that the plates were automatically transferred to Cytation 5 for fluorescence imaging of the test wells. A single 4x image was taken with the GFP and RFP channels to capture potential movement of the U-87 and fibroblast cells, respectively, into the original wound area. Plates were then transferred back to the BioSpa 8, and kinetic imaging cycles were repeated every 90 minutes for a total of 48 hours.

Analysis and results

Following capture, kinetic fluorescent images were pre-processed to remove background signal (Figure 12).

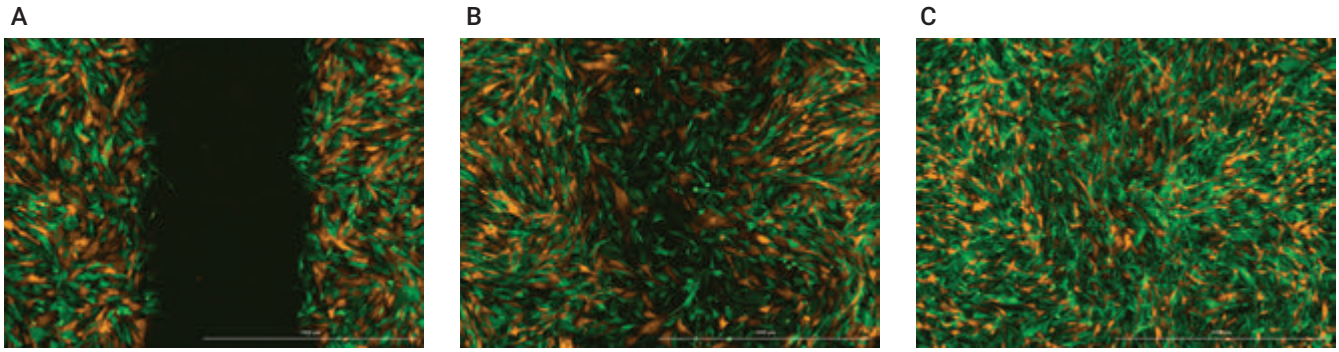

Figure 12. Fluorescent images of fibroblast and U-87 co-cultured wound healing. Kinetic images captured of uninhibited RFP expressing fibroblast and GFP expressing U-87 cell migration after (A) 0, (B) 18, and (C) 48 hour incubations.

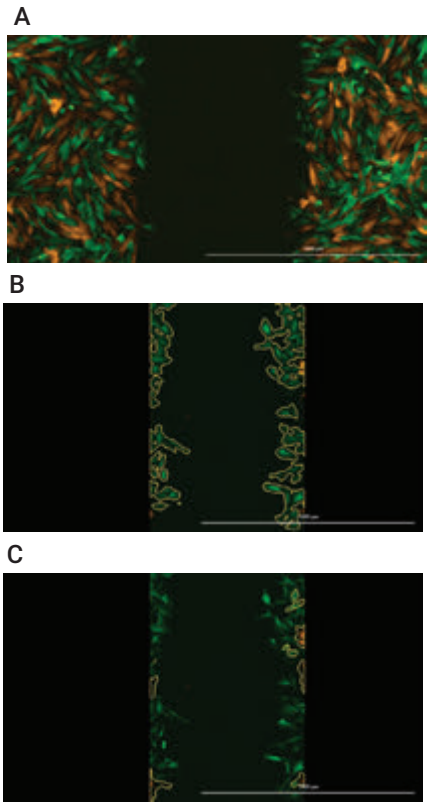

Figure 13. Cellular analysis of individual co-cultured cell types within created wound. (A) Overlaid fluorescent images of RFP expressing fibroblastsand GFP expressing U-87 cells immediately following wound creation. (B) Cellular analysis of GFP signal from U-87 cells post 3 hour incubation. (C) Cellular analysis of RFP signal from fibroblasts post 3 hour incubation.

Two separate cellular analysis steps were then performed to assess the migration characteristics of each included cell. However, as neither the fibroblasts or U-87 cells form a confluent monolayer on each side of the created wound, a new analysis method was incorporated. In the analysis step an image plug was applied covering the areas to the left and right of the wound created by AutoScratch, leaving only the cell-free zone. In this way only U-87 or fibroblast cell migration into the open, uncovered areas of the image was analyzed by using changes in the GFP or RFP signal, respectively (Figure 13).

Gen5 then automatically calculates the normalized fraction of cells within the original wound area, or wound confluence value. Kinetic wound confluence curves are then plotted to ascertain any possible differences between the cell migration patterns of the co-cultured cell models (Figure 14). When comparing the two kinetic curves for the first six hours following wound creation (Figure 14B), in addition to Gen5 generated maximum wound healing rates over that time, it is clear that the U-87 glioblastoma cells had a higher initial rate (404 μm^2/minute) of migration compared to the fibroblasts (122 μm^2/minute), which demonstrated relatively low migratory rates, particularly in the first four hours.

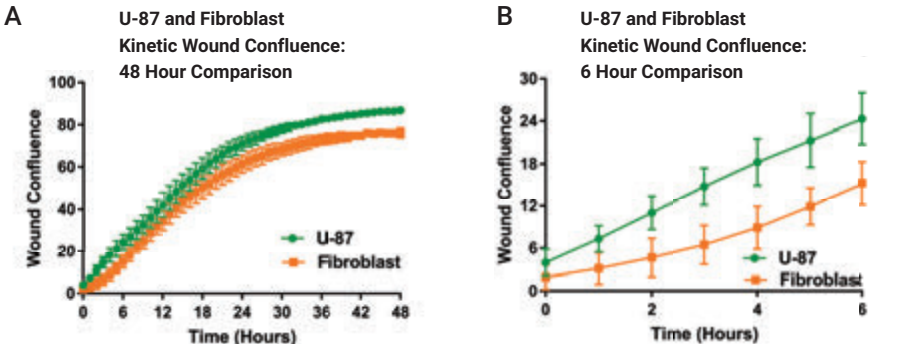

Figure 14. Uninhibited cell migration curves of co-cultured cell models. Kinetic wound confluence curves for GFP expressing U-87 cells and RFP expressing fibroblasts. Curves shown for (A) 48 hour; and (B) 6 hour incubations.

Recent publications using Agilent BioTek microscopes

1. Chen, Xuenan, et al. "Panax ginseng total protein promotes proliferation and secretion of collagen in NIH/3T3 cells by activating extracellular signal-related kinase pathway." *Journal of Ginseng Research*, 1 Mar. **2017**. Doi: 10.1016/j.jgr.2017.02.001.

2. Nanayakkara, Amila K., et al. "Prolonged Inhibition of P-Glycoprotein after Exposure to Chemotherapeutics Increases Cell Mortality in Multidrug Resistant Cultured Cancer Cells." *PLOS ONE, edited by Jed N. Lampe, vol. 14, no. 6,* June **2019**, *p. e0217940*. Doi: 10.1371/journal.pone.0217940.

3. Sultan, Ahmed S., et al. "Evaluation of the Antifungal and Wound-Healing Properties of a Novel Peptide-Based Bioadhesive Hydrogel Formulation." *Antimicrobial Agents and Chemotherapy, vol. 63, no. 10,* July **2019**, *pp. e00888-19, /aac/63/10/AAC.00888-19.atom.* Doi: 10.1128/AAC.00888-19.

Monitoring mitochondrial dynamics via live cell imaging

Assay principle

The cell-permeant MitoTracker probes contain a mildly thiol-reactive chloromethyl moiety for labeling mitochondria. MitoTracker Red CMXRos is a red-fluorescent dye that readily passes through cell membranes and accumulates in healthy, active mitochondria. If the mitochondria membrane is depolarized or inactive, the dye diffuses throughout the cell, and a decrease in signal is seen.

Method summary

HT-1080 cells were added to half area 96-well plates and allowed to attach. Cells were then stained with 10 µM Hoechst 33342 and 100 nM MitoTracker Red CMXRos for 20 minutes. The plate was then inserted into a Agilent BioTek imager to capture a single initial image prior to treatment using a 40x objective, the DAPI imaging channel to capture signal from the Hoechst 33342 probe, and the Texas Red channel to capture signal from the MitoTracker probe. The plate was then removed from the imager and washed to remove dye not taken into the cells. A titration of FCCP ranging from 10-0 µM, using serial 1:3 dilutions, was added to the wells, and the plate was placed back into the imager where kinetic fluorescent imaging took place every 5 minutes again using a 40x objective, and the DAPI and Texas Red imaging channels.

Analysis and results

Following capture, kinetic fluorescent images were pre-processed to remove background signal (Figure 15).

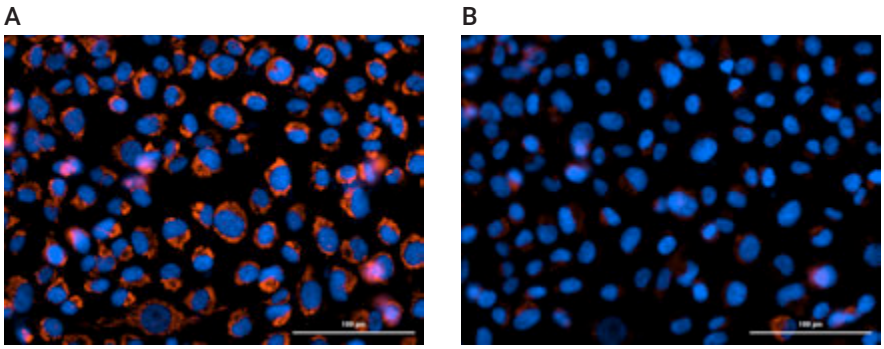

Figure 15. Overlaid pre-processed DAPI and Texas Red images before (A) and after (B) one hour 10 µM FCCP treatment, capturing Hoechst 33342 nuclear and MitoTracker probe signals, respectively.

Then using the change in signal in the DAPI channel, primary object masks were automatically placed around all cells in the image (Figure 16). Primary object masks were automatically placed around all cell nuclei using the DAPI channel.

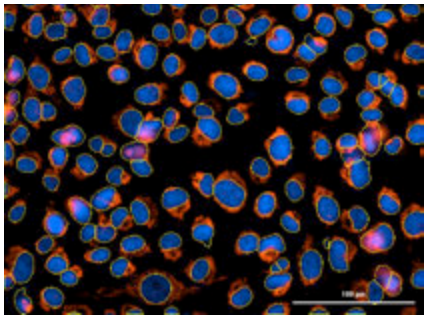

Figure 16. Overlaid pre-processed DAPI and Texas Red image showing primary object masks automatically applied using change in DAPI signal during cellular analysis.

Secondary masks were then generated, extending out from the primary mask to encompass the MitoTracker probe captured using the Texas Red imaging channel. (Figure 17A). Addition of FCCP, a strong ionophore and mitochondrial uncoupler, causes a loss of MitoTracker signal due to mitochondrial depolarization. Because the same delta signal threshold criteria is used for the analysis of all kinetic images, secondary mask area following a one hour treatment with 10 µM FCCP decreases dramatically (Figure 17B).

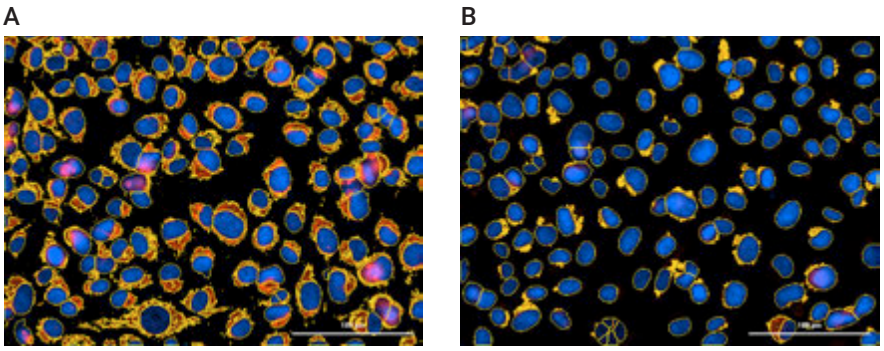

Figure 17. Overlaid preprocessed DAPI and Texas Red image showing primary and secondary object mask placement (A) prior to, and (B) following one hour 10 µM FCCP treatment.

Gen5 can then be used to create a ratio, expressed as a percentage, of the average area coverage at each timepoint during the kinetic to the original average area coverage. When plotted over time it becomes clear the effect that the concentration of FCCP is having on mitochondrial polarization (Figure 18).

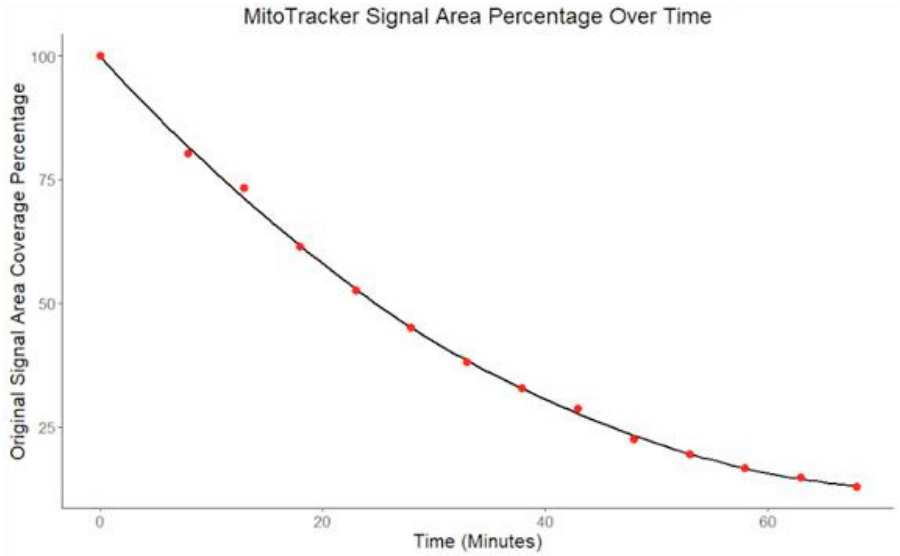

Figure 18. Graph of kinetic normalized average MitoTracker signal coverage during 10 µM FCCP treatment.

Finally, as previously described, Gen5 can calculate the area under kinetic curves, generating one total area value for the curve corresponding to each concentration of FCCP tested. These numbers can then be plotted in relation to the FCCP concentration to create an IC_{50} value of 4.2 µM, demonstrating the ability of the compound to interrupt mitochondrial polarization (Figure 19).

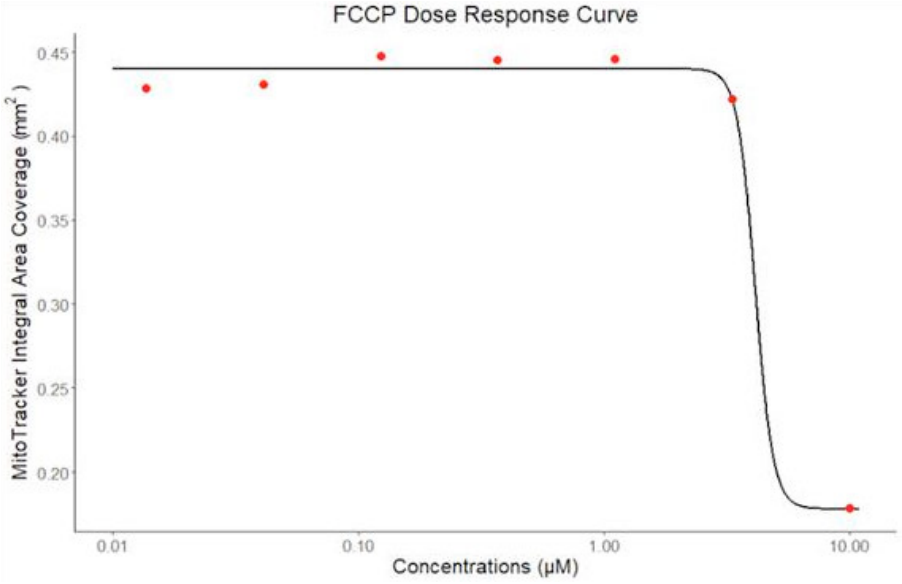

Figure 19. Graph of area under the curve values plotted in terms of FCCP concentration to determine compound effect on mitochondrial polarization.

Recent publications using Agilent BioTek microscopes

1. Martins, A. D., et al. "Ghrelin Acts as Energy Status Sensor of Male Reproduction by Modulating Sertoli Cells Glycolytic Metabolism and Mitochondrial Bioenergetics." *Molecular and Cellular Endocrinology, vol. 434,* Oct. **2016**, *pp. 199–209.* Doi: 10.1016/j.mce.2016.07.008.
2. Di Cristo, Francesca, et al. "Meldonium Improves Huntington's Disease Mitochondrial Dysfunction by Restoring Peroxisome Proliferator activated Receptor γ Coactivator 1α Expression." *Journal of Cellular Physiology, vol. 234, no. 6,* June **2019**, *pp. 9233–46.* Doi: 10.1002/jcp.27602.
3. Chen, Zongyan, et al. "The Roles of Mitochondria in Radiation-Induced Autophagic Cell Death in Cervical Cancer Cells." *Tumor Biology, vol. 37, no. 3,* Mar. **2016**, *pp. 4083–91.* Doi: 10.1007/s13277-015-4190-8.

Conclusion

We have demonstrated several live cell kinetic fluorescent assays using organelle-based or phentotypic probes or fluorescent proteins. Each of the assay workflows can be easily automated with Agilent BioTek imaging instrumentation and automation, including the Agilent BioTek BioSpa and Agilent BioTek AutoScratch. The combination of kinetic assay chemistries, and automated instrumentation can generate high-quality, accurate, reproducible results for a variety of research applications.

References

1. Dunn, Graham A., and Gareth E. Jones. "Cell Motility under the Microscope: Vorsprung Durch Technik." *Nature Reviews Molecular Cell Biology, vol. 5, no. 8,* Aug. **2004**, *pp. 667–72.* Doi: 10.1038/nrm1439.
2. Frischknecht, Freddy, et al. "Retrospective: Birth of the Cool - Imaging and Microbiology from Ibn al-Haytham to Jean Comandon." *Biotechnology Journal, vol. 4, no. 6*, June **2009**, *pp. 787–90.* Doi: 10.1002/biot.200900102.
3. Bertrand, Julien Y., et al. "Haematopoietic Stem Cells Derive Directly from Aortic Endothelium during Development." *Nature, vol. 464, no. 7285,* Mar. **2010**, *pp. 108–11*. Doi: 10.1038/nature08738.
4. Eilken, Hanna M., et al. "Continuous Single-Cell Imaging of Blood Generation from Haemogenic Endothelium." *Nature, vol. 457, no. 7231,* Feb. **2009**, *pp. 896–900.* Doi: 10.1038/nature07760.
5. Kissa, Karima, and Philippe Herbomel. "Blood Stem Cells Emerge from Aortic Endothelium by a Novel Type of Cell Transition." *Nature, vol. 464, no. 7285,* Mar. **2010**, *pp. 112–15.* Doi: 10.1038/nature08761.
6. Rieger, Michael A., et al. "Hematopoietic Cytokines Can Instruct Lineage Choice." *Science, vol. 325, no. 5937,* July **2009**, *pp. 217–18.* Doi: 10.1126/science.1171461.
7. Asami, Maki, et al. "The Role of Pax6 in Regulating the Orientation and Mode of Cell Division of Progenitors in the Mouse Cerebral Cortex." *Development, vol. 138, no. 23,* Dec. **2011**, *pp. 5067–78.* Doi: 10.1242/dev.074591.
8. Costa, Marcos R., et al. "Par-Complex Proteins Promote Proliferative Progenitor Divisions in the Developing Mouse Cerebral Cortex." *Development, vol. 135, no. 1,* Nov. **2007**, *pp. 11–22.* Doi: 10.1242/dev.009951.
9. Costa, Marcos R., et al. "Late Origin of Glia-Restricted Progenitors in the Developing Mouse Cerebral Cortex." *Cerebral Cortex, vol. 19, no. suppl_1,* July **2009**, *pp. i135–43.* Doi: 10.1093/cercor/bhp046.

10. Costa, Marcos R., et al. “Continuous Live Imaging of Adult Neural Stem Cell Division and Lineage Progression in Vitro.” *Development, vol. 138, no. 6,* Mar. **2011**, *pp. 1057–68.* Doi: 10.1242/dev.061663.

11. Henrickson, Sarah E., et al. “T Cell Sensing of Antigen Dose Governs Interactive Behavior with Dendritic Cells and Sets a Threshold for T Cell Activation.” *Nature Immunology, vol. 9, no. 3, Mar*. **2008**, *pp. 282–91.* Doi: 10.1038/ ni1559.

12. Junt, Tobias, et al. “Subcapsular Sinus Macrophages in Lymph Nodes Clear Lymph-Borne Viruses and Present Them to Antiviral B Cells.” *Nature, vol. 450, no. 7166,* Nov. **2007**, *pp. 110–14.* Doi: 10.1038/nature06287.

13. Sung, Jung Hwan, et al. “Chemokine Guidance of Central Memory T Cells Is Critical for Antiviral Recall Responses in Lymph Nodes.” *Cell, vol. 150, no. 6,* Sept. **2012**, pp. 1249–63. Doi: 10.1016/j.cell.2012.08.015.

14. Prasher, Douglas C., et al. “Primary Structure of the Aequorea Victoria Green-Fluorescent Protein.” *Gene, vol. 111, no. 2,* Feb. **1992**, *pp. 229–33.* Doi: 10.1016/0378-1119(92)90691-H.

15. Ai, Hui-wang, et al. “Exploration of New Chromophore Structures Leads to the Identification of Improved Blue Fluorescent Proteins †.” *Biochemistry, vol. 46, no. 20,* May **2007**, *pp. 5904–10.* Doi: 10.1021/bi700199g.

16. Cubitt, Andrew B., et al. “Understanding, Improving and Using Green Fluorescent Proteins.” *Trends in Biochemical Sciences, vol. 20, no. 11,* Nov. **1995**, *pp. 448–55.* Doi: 10.1016/S0968-0004(00)89099-4.

17. Heim, Roger, and Roger Y. Tsien. “Engineering Green Fluorescent Protein for Improved Brightness, Longer Wavelengths and Fluorescence Resonance Energy Transfer.” *Current Biology, vol. 6, no. 2,* Feb. **1996**, *pp. 178–82.* Doi: 10.1016/S0960-9822(02)00450-5.

18. Zhang, Jin, et al. “Creating New Fluorescent Probes for Cell Biology.” *Nature Reviews Molecular Cell Biology, vol. 3, no. 12,* Dec. **2002**, *pp. 906–18.* Doi: 10.1038/nrm976.

19. Sakaue-Sawano, Asako, et al. “Visualizing Spatiotemporal Dynamics of Multicellular Cell-Cycle Progression.” *Cell, vol. 132, no. 3,* Feb. **2008**, *pp. 487–98.* Doi: 10.1016/j.cell.2007.12.033.

20. Hepler, John R., and Alfred G. Gilman. “G Proteins.” *Trends in Biochemical Sciences, vol. 17, no. 10,* Oct. **1992**, *pp. 383–87.* Doi: 10.1016/0968-0004(92)90005-T.

21. Rajaram, Megha, et al. “System-Wide Analysis Reveals a Complex Network of Tumor-Fibroblast Interactions Involved in Tumorigenicity.” *PLoS Genetics, edited by Marshall S. Horwitz, vol. 9, no. 9,* Sept. **2013**, *p. e1003789*. Doi: 10.1371/journal.pgen.1003789.

Learn more:
www.agilent.com/lifesciences/biotek

Get answers to your technical questions and access resources in the Agilent Community:
community.agilent.com

Buy online:
www.agilent.com/chem/store

U.S. and Canada
1-800-227-9770
agilent_inquiries@agilent.com

Europe
info_agilent@agilent.com

Asia Pacific
inquiry_lsca@agilent.com

RA44173.6629282407

Published in the USA, February 1, 2021
5994-2567EN
AG052920_01

Agilent
Trusted Answers